An Overlapping Preconditioner for 2D Virtual Problems Posed in H(rot) with Irregular Subdomains

Juan G. Calvo, César Herrera, and Filánder A. Sequeira

1 Introduction

Given a bounded polygonal domain $\Omega \subset \mathbb{R}^2$, we seek $\boldsymbol{u} \in H_0(\mathrm{rot};\Omega)$ such that

$$a(\boldsymbol{u},\boldsymbol{v}) := \int_\Omega (\alpha \ \mathrm{rot}\ \boldsymbol{u}\ \mathrm{rot}\ \boldsymbol{v} + \beta \boldsymbol{u}\cdot\boldsymbol{v}) = \int_\Omega \boldsymbol{f}\cdot\boldsymbol{v} \quad \forall \boldsymbol{v} \in H_0(\mathrm{rot};\Omega), \tag{1}$$

where $\mathrm{rot}\ \boldsymbol{u} := \partial_{x_1}u_2 - \partial_{x_2}u_1$, $\boldsymbol{f} \in [L^2(\Omega)]^2$, and $\alpha,\beta \in L^\infty(\Omega)$ are positive functions that are uniformly bounded from below. The weak form (1) arises from implicit time integration of the eddy current model of Maxwell's equation [5] and is considered in several studies; see, e.g., [1, 13]. We recall that

$$H_0(\mathrm{rot};\Omega) := \left\{\boldsymbol{v} \in [L^2(\Omega)]^2 : \mathrm{rot}\,\boldsymbol{v} \in L^2(\Omega),\ \boldsymbol{v}\cdot\boldsymbol{t} = 0 \text{ on } \partial\Omega\right\},$$

where $\boldsymbol{t}$ denotes the unit tangential vector on $\partial\Omega$. The bilinear form $a(\cdot,\cdot)$ defined in (1) is obtained from the differential operator $\mathcal{L}\boldsymbol{u} := \mathbf{rot}\ (\alpha \mathrm{rot}\ \boldsymbol{u}) + \beta\boldsymbol{u}$, where $\mathbf{rot}\ q := \left(\partial_{x_2}q, -\partial_{x_1}q\right)^T$. The well-posedness of problem (1) can be established by a straightforward application of the Lax-Milgram lemma; for the sake of brevity we omit further details and refer to [15].

In this paper, we present a two-level overlapping Schwarz preconditioner for problem (1) discretized with finite or virtual element methods (FEM or VEM, respectively) in two dimensions. To the best of our knowledge, there are no theoretical

Juan G. Calvo
CIMPA – Escuela de Matemática, Universidad de Costa Rica, Costa Rica,
e-mail: juan.calvo@ucr.ac.cr

César Herrera
Purdue University, West Lafayette, IN 47907, e-mail: herre125@purdue.edu

Filánder A. Sequeira
Escuela de Matemática, Universidad Nacional, Heredia, Costa Rica,
e-mail: filander.sequeira@una.cr

results for preconditioning the linear system that arises from (1) when VEM are used. Our method allows us to handle irregular subdomains and general polygonal meshes, and applies to a broader range of material properties and subdomain geometries than previous studies.

First studies for problems posed in $H^1(\Omega)$ with FEM discretizations and irregular subdomains include [14, 17, 11], where discrete harmonic extensions are required for the construction of a coarse component of the preconditioner; for problems posed in $H(\mathrm{rot};\Omega)$ see [7, 8]. Such algorithms require us to solve a linear system on the fine mesh for each coarse function. The ideas introduced in [9, 10] allowed to extend standard Domain Decomposition Methods (DDM) from FEM to VEM for problems posed in $H^1(\Omega)$ in a natural way. Hence, we replace harmonic extensions by projectors onto polynomial spaces of degree at most k. In this variant, we need to solve a linear system with just $O(k^2)$ unknowns in order to construct a coarse function, reducing the complexity of the construction of coarse functions while preserving the dimension of the coarse space defined in [7] for FEM, which is equal to the number of interior subdomain edges. In this paper, we present such generalization for problems posed in $H(\mathrm{rot};\Omega)$.

In [7], a theoretical bound for the condition number κ of a two-level overlapping Schwarz preconditioner for FEM, based on discrete harmonic extensions, is given by

$$\kappa \leq C\left(1+\frac{H}{\delta}\right)\left(1+\log\frac{H}{h}\right),$$

where C only depends on α, β and some parameters related to the regularity of the subdomains. We observe similar results for our preconditioner when VEM and harmonic extensions are considered.

We remark that there are different DDM such as FETI-DP and BDDC methods; see [12, 8] for studies related to our problem. Nevertheless, the simplicity of implementing an overlapping additive Schwarz algorithm with competitive results gives relevance to our work.

The rest of this paper is organized as follows. We briefly describe the VEM for our model problem (1) in Section 2. We then describe the two-level overlapping additive Schwarz and the definition of our coarse space with detail in Section 3. Finally, some numerical results and conclusions are included in Section 4.

2 The virtual element method

We briefly describe a virtual element scheme for problem (1). Given an integer $\ell \geq 0$, let $\mathbb{P}_\ell(\mathcal{D})$ denote the space of polynomials defined in $\mathcal{D}$ of total degree at most ℓ. Let $\{\mathcal{T}_h\}_{h>0}$ be a family of decompositions of Ω into polygonal elements. We assume that there exists a constant $C_{\mathcal{T}} > 0$ such that for each decomposition $\mathcal{T}_h$ and for each $E \in \mathcal{T}_h$ it holds that (see, e.g., [6, Section 3.2] and [4, Section 2]):

1. the ratio between the shortest edge and the diameter h_E is bigger than $C_{\mathcal{T}}$, and
2. E is star-shaped with respect to a ball of radius $C_{\mathcal{T}} h_E$ and center $\boldsymbol{x}_E \in E$.

The lowest-order conforming Nédélec first-type local space

$$N_0^E := \{\boldsymbol{v} \in [\mathbb{P}_1(E)]^2 : \boldsymbol{v} = (-bx_2 + a_1, bx_1 + a_2)^T, a_1, a_2, b \in \mathbb{R}\}$$

is typically used for the discretization of (1) with triangular meshes; see [12, 7, 8]. For general polygonal meshes, we replace the Nédélec space N_0^E by the lowest-order local virtual element space W_0^E, defined as

$$W_0^E := \left\{\boldsymbol{v} \in [L^2(E)]^2 : \boldsymbol{v} \cdot \boldsymbol{t}|_e \in \mathbb{P}_0(e) \forall e \in \partial E, \operatorname{rot} \boldsymbol{v}, \operatorname{div} \boldsymbol{v} \in \mathbb{P}_0(E), \int_E \boldsymbol{v} \cdot \boldsymbol{x}_E = 0\right\}$$

where $e \in \partial E$ represents an edge of E, $\boldsymbol{x}_E = \boldsymbol{x} - \boldsymbol{b}_E$, and $\boldsymbol{b}_E$ is the barycenter of E; see [4, eq. (28)]. The degrees of freedom of a virtual function $\boldsymbol{v} \in W_0^E$ can be chosen as the moments $\lambda^e(\boldsymbol{v}) = \frac{1}{|e|}\int_e \boldsymbol{v} \cdot \boldsymbol{t}$ for each edge $e \in \partial E$, similar as what is done when Nédélec elements are used; see, e.g., [3, eq. (3.13)]. We remark that $\operatorname{rot} \boldsymbol{v} = \frac{1}{|E|}\int_E \operatorname{rot} \boldsymbol{v} = \frac{1}{|E|}\int_{\partial E} \boldsymbol{v} \cdot \boldsymbol{t} = \frac{1}{|E|}\sum_{e\in\partial E} |e|\lambda^e(\boldsymbol{v})$, and therefore we can compute the rotor of $\boldsymbol{v} \in W_0^E$ from its degrees of freedom. Thus, the term $\int_E \alpha \operatorname{rot} \boldsymbol{u} \operatorname{rot} \boldsymbol{v}$ of the bilinear form can be computed and we only require to modify the mass matrix. Given $\boldsymbol{v} \in [L^2(E)]^2$, let $\Pi_1^E : [L^2(E)]^2 \to [\mathbb{P}_1(E)]^2$ be the orhogonal projector given by

$$\int_E \Pi_1^E \boldsymbol{v} \cdot \boldsymbol{p} = \int_E \boldsymbol{v} \cdot \boldsymbol{p} \quad \forall \boldsymbol{p} \in [\mathbb{P}_1(E)]^2. \tag{2}$$

We remark that Π_1^E is computable for functions in W_0^E only knowing its degrees of freedom; we omit details and refer to [2, Remark 3]. For the mass-term, we then replace $\boldsymbol{v}$ by $\Pi_1^E \boldsymbol{v}$ in the local bilinear form. Therefore, as it is standard in VEM, a stabilizing term is required, which is defined as

$$s_E(\boldsymbol{w}, \boldsymbol{v}) := h_E \sum_{e\in\partial E} \int_e (\boldsymbol{w} \cdot \boldsymbol{t})(\boldsymbol{v} \cdot \boldsymbol{t}) \quad \forall \boldsymbol{w}, \boldsymbol{v} \in V_0(E);$$

see [4, Theorem A.2] and [3, eq. (4.8)] for further details. We then consider the local bilinear form

$$a_h^E(\boldsymbol{w}, \boldsymbol{v}) := \int_E \left(\alpha \operatorname{rot} \boldsymbol{w} \operatorname{rot} \boldsymbol{v} + \beta \Pi_1^E \boldsymbol{w} \cdot \Pi_1^E \boldsymbol{v}\right) + s_E\left(\boldsymbol{w} - \Pi_1^E \boldsymbol{w}, \boldsymbol{v} - \Pi_1^E \boldsymbol{v}\right)$$

for $\boldsymbol{w}, \boldsymbol{v} \in W_0^E$. The global virtual element space $V_h \subset H_0(\operatorname{rot}; \Omega)$ is then given by

$$V_h := \left\{\boldsymbol{v} \in H_0(\operatorname{rot}; \Omega) : \boldsymbol{v}|_E \in W_0^E \ \forall E \in \mathcal{T}_h\right\}, \tag{3}$$

and, as usual, the global bilinear form is obtained by assembling the local bilinear forms $a_h^E(\cdot, \cdot)$. We then define the virtual element scheme associated to (1): find $\boldsymbol{u}_h \in V_h$ such that

$$\sum_{E\in\mathcal{T}_h} a_h^E(\boldsymbol{u}_h,\boldsymbol{v}_h) = \sum_{E\in\mathcal{T}_h}\int_E \boldsymbol{f}\cdot\Pi_1^E\boldsymbol{v}_h \quad \forall\,\boldsymbol{v}_h\in V_h.$$

This problem is well-posed and standard estimates for the approximated solution can be obtained; for the sake of brevity we omit such details.

3 Overlapping Schwarz methods

In this section, we briefly describe two-level overlapping methods; see [16, Chapter 3] for further details. We partition the domain Ω into N non-overlapping subdomains $\{\Omega_i\}_{i=1}^N$ of diameter H_i which are the union of elements of $\mathcal{T}_h$. Subdomains are assumed to satisfy the same assumptions as the elements on the fine mesh; this implies that they are simply connected and the number of edges of each subdomain is uniformly bounded. The edges on this decomposition are denoted by e^H, which correspond to edges of the polygons Ω_i. We then construct overlapping subdomains $\Omega_i'\supset\Omega_i$ by adding layers of elements that are external to Ω_i, and we will denote by δ_i the minimum width of the region $\Omega_i'\setminus\Omega_i$.

We consider the usual local virtual spaces V_i, $1\le i\le N$, defined by

$$V_i := \left\{\boldsymbol{v}\in H_0(\mathrm{rot}\,;\Omega_i') : v|_E\in W_0^E\ \forall\, E\subset\Omega_i'\right\}.$$

Thus, the degrees of freedom of a function $\boldsymbol{v}_i\in V_i$ are $\lambda^e(\boldsymbol{v}_i)$ at the fine edges e that are in the interior of Ω_i'. We also consider the natural operators $R_i^T : V_i\to V_h$ given by the zero extension from the subdomain Ω_i' to Ω, $1\le i\le N$.

We can define the coarse space V_0 as the virtual element space (3) defined on the coarse mesh $\{\Omega_i\}_{i=1}^N$. Nevertheless, its dimension can be an inconvenience for parallel implementations in the presence of irregular subdomains with too many edges; see Figure 1. Instead, for each subdomain edge $\mathcal{E}^{ij}$ (defined as the interior of $\overline{\Omega}_i\cap\overline{\Omega}_j$), we define a coarse function $\boldsymbol{c}_{\mathcal{E}}\in V_0$ by defining its degrees of freedom of V_0. We set $\lambda^{e^H}(\boldsymbol{c}_{\mathcal{E}}) = \boldsymbol{d}_{\mathcal{E}}\cdot\boldsymbol{t}_{e^H}$ for every edge e^H in $\mathcal{E}$, and $\lambda^{e^H}(\boldsymbol{c}_{\mathcal{E}}) = 0$ otherwise. Here, $\boldsymbol{d}_{\mathcal{E}}$ denotes a unit vector in the direction between the endpoints of $\mathcal{E}$, and $\boldsymbol{t}_{e^H}$ is the unit tangent vector of e^H. The reduced coarse space V_0^R is then defined as the span of these coarse basis functions $\boldsymbol{c}_{\mathcal{E}}$. We remark that the dimension of V_0^R is equal to the number of subdomain edges, similar as in [7, 8, 12].

In order to define an operator $R_0^T : V_0^R\subseteq V_0\to V_h$ that approximates functions in the coarse space by elements in V_h, we can consider discrete harmonic extensions as in [7], for which a generalization for VEM can be established. Nevertheless, we can avoid discrete harmonic extensions by approximating virtual functions in V_0^R in the interior of subdomains by polynomials as follows. Consider the high-order virtual spaces of order $k\in\mathbb{N}$, defined on the coarse mesh, as the set

$$V_0^k = \{\boldsymbol{v}\in H_0(\mathrm{rot}\,;\Omega) : \boldsymbol{v}|_{\Omega_i}\in W_k^{\Omega_i}\ \forall i\in\{1,2,\ldots,N\}\},$$

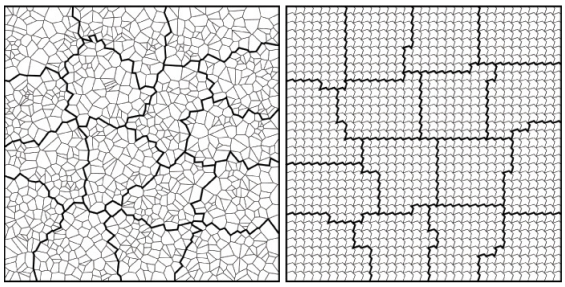

Fig. 1 (left) Voronoi mesh and (right) non-convex mesh with $N = 16$ irregular subdomains. Subdomains have, in average, 45 and 55 edges for the Voronoi and non-convex meshes, respectively.

where $W_k^{\Omega_i}$ is defined as the set

$$\left\{\boldsymbol{v} \in [L^2(\Omega_i)]^2 \colon \boldsymbol{v} \cdot \boldsymbol{t}|_{e^H} \in \mathbb{P}_k(e^H) \forall e^H \in \partial\Omega_i, \operatorname{rot} \boldsymbol{v} \in \mathbb{P}_k(\Omega_i), \operatorname{div} \boldsymbol{v} \in \mathbb{P}_{k-1}(\Omega_i)\right\}$$

Following [2, Section 3.2], the local degrees of freedom for $\boldsymbol{v} \in W_k^{\Omega_i}$ can be chosen as

$$\begin{aligned} m_q^{e^H}(\boldsymbol{v}) &:= \int_{e^H} (\boldsymbol{v} \cdot \boldsymbol{t})\, q \qquad \forall\, q \in \mathbb{P}_k(e^H)\,, \forall\, e^H \in \partial\Omega_i\,, \\ m_{p,\mathrm{rot}}^{\Omega_i}(\boldsymbol{v}) &:= \int_{\Omega_i} (\operatorname{rot} \boldsymbol{v})\, p \qquad \forall\, p \in \mathbb{P}_k(\Omega_i) \setminus \{1\}\,, \\ m_{p,\mathrm{div}}^{\Omega_i}(\boldsymbol{v}) &:= \int_{\Omega_i} (\boldsymbol{v} \cdot \boldsymbol{x}_{\Omega_i})\, p \qquad \forall\, p \in \mathbb{P}_{k-1}(\Omega_i)\,, \end{aligned}$$

which are unisolvent; see [2, Proposition 3.3]. It is clear that $V_0^R \subseteq V_0 \subseteq V_0^k$. For every coarse function $\boldsymbol{c}_{\mathcal{E}^{ij}} \in V_0^R$, we seek the degrees of freedom of the function $\widetilde{\boldsymbol{c}}_{\mathcal{E}^{ij}} \in V_0^k$, with the same degrees of freedom of $\boldsymbol{c}_{\mathcal{E}}$ on the interface, such that

$$\sum_{E \in \Omega_l} a_h^E(I^h(\Pi_k^{\Omega_l}\widetilde{\boldsymbol{c}}_{\mathcal{E}^{ij}}), I^h(\Pi_k^{\Omega_l}\widetilde{\boldsymbol{c}}_{\mathcal{E}^{ij}})) \tag{4}$$

is minimum for $l \in \{i, j\}$, where $\boldsymbol{w} = I^h\boldsymbol{v} \in V_h$ is the usual interpolant given by the condition $\lambda^e(\boldsymbol{v} - \boldsymbol{w}) = 0$ for all edge e, and $\Pi_k^{\Omega_l} : [L^2(\Omega_l)]^2 \to [\mathbb{P}_k(\Omega_l)]^2$ is the orthogonal projector onto Ω_l; see (2) for the case $k = 1$. The degrees of freedom of $\widetilde{\boldsymbol{c}}_{\mathcal{E}}$ given by $m_q^{e^H}(\widetilde{\boldsymbol{c}}_{\mathcal{E}})$ and $m_{p,\mathrm{rot}}^{\Omega_i}(\widetilde{\boldsymbol{c}}_{\mathcal{E}})$ are known and can be computed from $\boldsymbol{c}_{\mathcal{E}}$. Since $\int_{\Omega_i}(\boldsymbol{v} \cdot \boldsymbol{x}_{\Omega_i}) = 0$, the remaining degrees of freedom can be obtained just by solving a linear system with $k(k+1)/2 - 1$ equations for each subdomain with $\mathcal{E}$ on its boundary, obtained by directly computing the critical points of (4). For the sake of brevity we omit details and refer to [9] that includes how to obtain this linear system. Preserving degrees of freedom on the interface guarantees continuity across the interface when we interpolate coarse functions to the fine mesh. We then define $R_0^T\boldsymbol{c}_{\mathcal{E}} \in V_h$ by setting:

(a') $\lambda^e(R_0^T\boldsymbol{c}_{\mathcal{E}}) = \lambda^e(\boldsymbol{c}_{\mathcal{E}})$ if e is an edge on the interface;
(b') $\lambda^e(R_0^T\boldsymbol{c}_{\mathcal{E}}) = \lambda^e(\Pi_k^{\Omega_l}\widetilde{\boldsymbol{c}}_{\mathcal{E}})$ if e is an interior edge of Ω_l;
(c') $\lambda^e(R_0^T\boldsymbol{c}_{\mathcal{E}}) = 0$ otherwise;

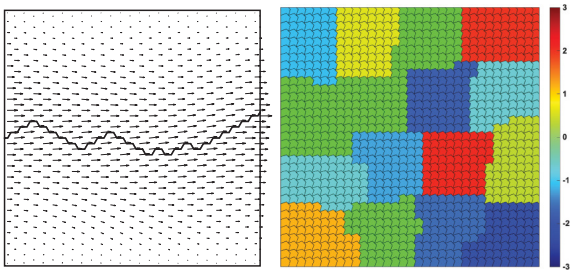

Fig. 2 (left) $R_0^T \boldsymbol{c}_{\mathcal{E}}$ for an irregular edge $\mathcal{E}$, evaluated in the interior of each subdomain by interpolating $\Pi_6^{\Omega_i}$ for $i \in \{1, 2\}$. (right) A discontinuous coefficient β varying from $\beta = 10^3$ (red) to $\beta = 10^{-3}$ (blue).

see Figure 2 where we show $R_0^T \boldsymbol{c}_{\mathcal{E}}$ for a given subdomain edge $\mathcal{E}$. We finally consider the two-level additive overlapping Schwarz preconditioner

$$P_{ad} := \sum_{i=0}^{N} P_i = A_{ad}^{-1} A, \text{ with } A_{ad}^{-1} = \sum_{i=0}^{N} R_i^T (R_i A R_i^T)^{-1} R_i, \tag{5}$$

where we consider exact solvers for each subspace for simplicity; see [16, Chap. 2].

4 Numerical results and conclusions

We present numerical results for the two-level additive overlapping Schwarz preconditioner (5). We solve the resulting linear systems using the preconditioned conjugate gradient method to a relative residual tolerance of 10^{-6}. We estimate the condition number $\kappa(P_{ad})$ and compute the number of iterations I_k (for spaces of degree k) and $I_{\mathcal{H}}$ (for the coarse space based on discrete harmonic extensions)

Table 1 Number of iterations I and condition number κ (in parenthesis) with Voronoi meshes and N METIS subdomains. I_3, I_6 and $I_{\mathcal{H}}$ correspond to $k = 3$, $k = 6$ and discrete harmonic extensions, respectively. $N_{\mathcal{E}}$ is the dimension of the coarse space.

		$\beta = 10^{-3}$			$\beta = 1$			$\beta = 10^{3}$		
	$N_{\mathcal{E}}$	$I_3\,(\kappa)$	$I_6\,(\kappa)$	$I_{\mathcal{H}}\,(\kappa)$	$I_3\,(\kappa)$	$I_6\,(\kappa)$	$I_{\mathcal{H}}\,(\kappa)$	$I_3\,(\kappa)$	$I_6\,(\kappa)$	$I_{\mathcal{H}}\,(\kappa)$
N		Test 1: $H/h = 8$, $H/\delta = 2$, $\alpha = 1$								
8^2	161	38 (47.5)	31 (23.9)	21 (7.7)	35 (38.5)	22 (10.5)	20 (7.2)	18 (7.3)	18 (7.3)	18 (7.3)
12^2	389	58 (112)	49 (79.0)	24 (9.4)	55 (95.7)	33 (20.3)	21 (8.0)	20 (8.3)	19 (8.2)	19 (8.2)
16^2	709	73 (201)	66 (181)	23 (9.3)	69 (163)	51 (51.6)	21 (8.0)	20 (7.9)	20 (7.9)	20 (7.9)
20^2	1128	90 (328)	84 (289)	25 (9.9)	84 (262)	68 (132)	22 (8.4)	20 (8.4)	20 (8.0)	20 (8.0)
H/δ		Test 2: $H/h = 32$, $N = 16$, $\alpha = 1$								
4	33	33 (25.4)	30 (24.1)	19 (6.1)	31 (22.8)	28 (19.8)	18 (6.0)	16 (5.1)	15 (5.1)	15 (5.1)
8	33	43 (58.3)	39 (52.3)	21 (7.5)	40 (49.5)	37 (35.6)	20 (7.0)	15 (4.8)	15 (4.9)	15 (5.0)
16	33	57 (136)	56 (124)	24 (12.7)	53 (100)	49 (65.7)	23 (13.0)	16 (6.1)	16 (6.1)	16 (6.0)
32	33	82 (300)	81 (300)	35 (28.6)	73 (166)	62 (101)	32 (23.0)	20 (8.6)	20 (8.4)	19 (7.8)
H/h		Test 3: $N = 16$, $H/\delta = 4$, $\alpha = 1$								
8	33	32 (32.6)	24 (12.4)	19 (7.2)	30 (22.4)	19 (6.9)	18 (7.0)	14 (5.4)	14 (5.3)	14 (5.3)
16	34	31 (26.8)	29 (26.1)	18 (6.1)	30 (22.9)	27 (14.1)	18 (5.8)	15 (5.1)	15 (5.0)	15 (5.1)
32	33	33 (25.4)	30 (24.1)	19 (6.1)	31 (22.8)	28 (19.8)	18 (6.0)	16 (5.1)	15 (5.1)	15 (5.1)
64	33	34 (22.6)	32 (22.6)	18 (5.5)	32 (21.6)	31 (19.3)	18 (5.5)	14 (5.3)	16 (5.1)	16 (5.1)

Table 2 Number of iterations I and condition number κ (in parenthesis) with non-convex meshes and N METIS subdomains. I_3, I_6 and $I_{\mathcal{H}}$ correspond to $k = 3, k = 6$ and discrete harmonic extensions, respectively. $N_{\mathcal{E}}$ is the dimension of the coarse space.

		$\beta = 10^{-3}$			$\beta = 1$			$\beta = 10^{3}$		
N	$N_{\mathcal{E}}$	$I_3\,(\kappa)$	$I_6\,(\kappa)$	$I_{\mathcal{H}}\,(\kappa)$	$I_3\,(\kappa)$	$I_6\,(\kappa)$	$I_{\mathcal{H}}\,(\kappa)$	$I_3\,(\kappa)$	$I_6\,(\kappa)$	$I_{\mathcal{H}}\,(\kappa)$
		Test 1: $H/h = 8$, $H/\delta = 2$, $\alpha = 1$								
8^2	158	38 (54.0)	28 (17.3)	20 (8.0)	36 (36.9)	21 (7.8)	19 (6.7)	20 (10.1)	20 (10.1)	20 (10.1)
12^2	379	57 (130)	45 (66.1)	21 (7.4)	53 (81.6)	29 (13.7)	20 (7.1)	23 (13.5)	23 (13.6)	22 (13.5)
16^2	699	76 (261)	61 (136)	21 (7.7)	69 (139)	34 (21.2)	20 (7.2)	24 (16.4)	24 (16.1)	24 (16.2)
20^2	1109	93 (537)	82 (265)	23 (8.3)	83 (245)	45 (38.3)	21 (8.5)	27 (20.9)	27 (20.7)	27 (20.9)
H/δ		Test 2: $H/h = 32$, $N = 16$, $\alpha = 1$								
4	33	33 (30.7)	30 (28.7)	18 (6.4)	31 (24.0)	29 (17.7)	17 (5.5)	15 (5.1)	15 (5.1)	15 (5.0)
8	33	43 (80.4)	42 (73.7)	22 (8.2)	42 (49.5)	35 (29.8)	20 (7.9)	17 (8.0)	17 (8.0)	16 (7.9)
16	33	56 (129)	57 (139)	26 (11.4)	52 (70.3)	45 (41.4)	24 (12.0)	21 (12.8)	21 (12.8)	20 (12.7)
32	33	78 (297)	78 (304)	34 (21.9)	67 (112)	55 (62.7)	32 (20.6)	30 (28.4)	30 (28.4)	29 (29.4)
H/h		Test 3: $N = 16$, $H/\delta = 4$, $\alpha = 1$								
8	33	31 (29.6)	23 (10.7)	18 (6.4)	27 (19.5)	18 (6.4)	17 (5.7)	19 (11.4)	19 (11.3)	19 (11.7)
16	31	31 (30.8)	29 (27.7)	18 (6.0)	29 (20.2)	23 (10.0)	17 (5.8)	16 (7.7)	16 (7.7)	16 (7.7)
32	33	33 (30.7)	30 (28.7)	18 (6.4)	31 (24.0)	29 (17.7)	17 (5.5)	15 (5.0)	15 (5.1)	15 (5.0)
64	33	38 (39.5)	33 (29.8)	19 (6.1)	35 (25.2)	31 (20.9)	18 (5.7)	16 (4.9)	16 (5.1)	15 (5.0)

Table 3 Number of iterations I and condition number κ (in parenthesis) with non-convex meshes and discontinuous values for β as in Figure 2. I_6 and $I_{\mathcal{H}}$ correspond to $k = 6$ and discrete harmonic extensions, respectively. $N_{\mathcal{E}}$ is the dimension of the coarse space.

N	$N_{\mathcal{E}}$	$I_6\ (\kappa)$	$I_{\mathcal{H}}\ (\kappa)$
8^2	158	20 (10.1)	20 (10.1)
12^2	379	23 (13.6)	22 (13.5)
16^2	699	24 (16.1)	24 (16.2)
20^2	1109	27 (20.7)	27 (20.9)

H/h	$N_{\mathcal{E}}$	$I_6\ (\kappa)$	$I_{\mathcal{H}}\ (\kappa)$
8	33	19 (11.3)	19 (11.7)
16	31	16 (7.7)	16 (7.7)
32	33	15 (5.1)	15 (5.0)
64	33	16 (5.1)	15 (5.0)

for each experiment; see results in Tables 1 and 2. We include different values for $\beta \in \{10^{-3}, 1, 10^3\}$ since previous bounds depend on the parameters α and β. We confirm the linear growth in the condition number as we increase H/δ and we observe no significant dependence on the parameter H/h. We observe that the coarse space based on discrete harmonic extensions is numerically scalable, and for small values of β the scalability is impaired when polynomial spaces are used. We remark that for the case of triangular meshes and square subdomains, our method recovers the same spaces as in [7]. We also include numerical results where β is piecewise constant on each subdomain; see Table 3 and Figure 2.

The theoretical bound for the condition number of the preconditioned system is in progress, where we have been able to obtain certain bounds for the coarse component of a decomposition for $\boldsymbol{u} \in V_h$, without considering Helmholtz decompositions as in [7]. There is also interest of implementing these ideas in 3D problems, in order to compare numerical results and running times with previous preconditioners. We also remark that similar results will hold for two-dimensional problems posed in $H(\mathrm{div}; \Omega)$, since two-dimensional Raviart-Thomas elements correspond to a 90° rotation of the elements considered in this paper.

Acknowledgements The authors gratefully acknowledges the institutional support for the project B8290 subscribed to *Vicerrectoría de Investigación, Universidad de Costa Rica*, and *Universidad Nacional, Costa Rica*, through the project 0140-20.

References

1. Beck, R., Hiptmair, R., Hoppe, R. H. W., and Wohlmuth, B. Residual based a posteriori error estimators for eddy current computation. *ESAIM: Math. Model. Numer. Anal.* **34**, 159–182 (2000).
2. Beirão da Veiga, L., Brezzi, F., Dassi, F., Marini, L., and Russo, A. Virtual element approximation of 2D magnetostatic problems. *Comput. Methods Appl. Mech. Eng.* **327**, 173–195 (2017).
3. Beirão da Veiga, L., Brezzi, F., Dassi, F., Marini, L., and Russo, A. Lowest order virtual element approximation of magnetostatic problems. *Comput. Methods Appl. Mech. Eng.* **332**, 343–362 (2018).
4. Beirão da Veiga, L. and Mascotto, L. Interpolation and stability properties of low-order face and edge virtual element spaces. *IMA J. Numer. Anal.* (2022).
5. Bossavit, A. Discretization of electromagnetic problems: The generalized finite differences approach. *Handb. Numer. Anal.* **13**, 105–197 (2005).
6. Cáceres, E. and Gatica, G. N. A mixed virtual element method for the pseudostress-velocity formulation of the Stokes problem. *IMA J. Numer. Anal.* **37**(1), 296–331 (2017).
7. Calvo, J. G. A two-level overlapping Schwarz method for $H(\mathrm{curl})$ in two dimensions with irregular subdomains. *Electron. Trans. Numer. Anal.* **44**, 497–521 (2015).
8. Calvo, J. G. A BDDC algorithm with deluxe scaling for $H(\mathrm{curl})$ in two dimensions with irregular subdomains. *Math. Comp.* **85**(299), 1085–1111 (2016).
9. Calvo, J. G. On the approximation of a virtual coarse space for domain decomposition methods in two dimensions. *Math. Models Methods Appl. Sci.* **28**(7), 1267–1289 (2018).
10. Calvo, J. G. An overlapping Schwarz method for virtual element discretizations in two dimensions. *Comput. Math. Appl.* **77**(4), 1163–1177 (2019).
11. Dohrmann, C. and Widlund, O. An alternative coarse space for irregular subdomains and an overlapping Schwarz algorithm for scalar elliptic problems in the plane. *SIAM J. Numer. Anal.* **50**, 2522–2537 (2012).
12. Dohrmann, C. R. and Widlund, O. B. An iterative substructuring algorithm for two-dimensional problems in $H(\mathrm{curl})$. *SIAM J. Numer. Anal.* **50**(3), 1004–1028 (2012).
13. Hiptmair, R. and Xu, J. Nodal auxiliary space preconditioning in $H(\mathrm{curl})$ and $H(\mathrm{div})$ spaces. *SIAM J. Numer. Anal.* **45**, 2483–2509 (2007).
14. Klawonn, A., Rheinbach, O., and Widlund, O. An analysis of a FETI-DP algorithm on irregular subdomains in the plane. *SIAM J. Numer. Anal.* **46**, 2484–2504 (2008).
15. Schöberl, J. Numerical methods for Maxwell equations. https://www.asc.tuwien.ac.at/ schoeberl/wiki/lva/notes/maxwell.pdf (2009). Accessed: 2022-11-22.
16. Toselli, A. and Widlund, O. *Domain decomposition methods-algorithms and theory*, *Springer Ser. Comput. Math.*, vol. 34. Springer (2005).
17. Widlund, O. Accommodating irregular subdomains in domain decomposition theory. In: Bercovier, M., Gander, M. J., Kornhuber, R., and Widlund, O. (eds.), *Domain Decomposition Methods in Science and Engineering XVIII*, *Lecture Notes in Computational Science and Engineering*, vol. 70, 87–98. Springer-Verlag (2009).